Arene Osmium Complexes with Ethacrynic Acid-Modified Ligands: Synthesis, Characterization and Evaluation of Intracellular Glutathione S-transferase Inhibition and Antiproliferative Activity

Gabriele Agonigi,[a] Tina Riedel,[b] M. Pilar Gay,[c] Lorenzo Biancalana,[a] Enrique Oñate,[c] Paul J. Dyson,[b] Guido Pampaloni,[a] Emilia Păunescu,[b] Miguel A. Esteruelas,[c,] Fabio Marchetti [a,*]*

[a]*Dipartimento di Chimica e Chimica Industriale, Università di Pisa, Via G. Moruzzi 13, I-56124 Pisa, Italy.*

[b]*Institut des Sciences et Ingénierie Chimiques, Ecole Polytechnique Fédérale de Lausanne (EPFL), CH-1015 Lausanne, Switzerland.*

[c]*Departamento de Química Inorgánica, Instituto de Síntesis Química y Catálisis Homogénea (ISQCH), Centro de Innovación en Química Avanzada (ORFEO-CIQA), Universidad de Zaragoza-CSIC, 50009 Zaragoza, Spain.*

Abstract

Four arene osmium complexes were prepared containing derivatives of ethacrynic acid, a potent inhibitor of glutathione S-transferases, either by direct coordination or via N- or P-donor ligands. The complexes were characterized by spectroscopic and analytical methods and, for Os(η^6-*p*-cymene)(acetylacetonato)(2-(2,3-dichloro-4-(2-ethylenebutanoyl)phenoxy) acetato) and Os(η^6-*p*-cymene)Cl_2(2-(2-(2,3-dichloro-4-(2-methylenebutanoyl)phenoxy)acetoxy)ethyl nicotinato), by single-crystal X-ray diffraction. The cytotoxicity of the complexes towards the human ovarian cancer cells and non-tumorous human embryonic kidney cells was investigated, and two of the complexes, for which ruthenium analogues are known, helped to delineate the influence of the metal ion. Inhibition studies of intracellular glutathione *S*-transferases (GSTs - detoxification enzymes implicated in drug resistance) indicate that the observed cytotoxicity of the complexes involves GST inhibition, as well as other targets following dissociation of the ethacrynic acid group from the osmium(II) ion.

Keywords: bioorganometallic chemistry, bioinorganic chemistry, metal-based drugs, arene osmium complexes, ethacrynic acid.

Introduction

Arene ruthenium(II) complexes have been intensively investigated as possible anticancer agents,[1] and especially those complexes containing 1,3,5-triaza-7-phosphatricyclo[3.3.1.1]decane (RAPTA complexes) and ethylene-1,2-diamine as ligands show promising antitumor properties.[2] On account of the proximity of ruthenium and osmium in the same group of the periodic table, a variety of osmium(II) derivatives have been considered as a natural extension of this research.[3] In particular, arene osmium complexes usually exhibit slower rates for ligands exchange than the ruthenium analogues, a desirable property providing increased drug stability under physiological conditions.[4]

One of the common approaches aimed at improving the efficacy of metal drugs consists of incorporating an organic fragment with a complementary biological function.[5] This strategy has already been applied also to various anticancer arene ruthenium(II) and osmium(II) complexes, which have been functionalized with biologically active moieties such as 3-hydroxyflavones,[6] lapachol,[7] paullones,[8] and lonidamine.[9]

It has previously been shown that ethacrynic acid, originally developed as an inhibitor of glutathione *S*-transferases (GSTs, a family of cytosolic detoxification enzymes associated with drug resistance), potentiates the cytotoxic effect of several chemotherapeutic agents, including cisplatin.[10] Consequently, in an attempt to overcome drug resistance, ethacrynic acid has been tethered to the ruthenium(II)-arene framework *via* two distinct synthetic approaches, i.e. the modification of the arene ligand [11] and the introduction via an appropriate monodentate ligand. In this respect, ethacrynic acid-functionalized imidazole,[12] pyridine and triphenylphosphine-type [13] ligands have been used (Figure 1). Also ruthenium(III), platinum(II) and platinum(IV) complexes with ethacrynic acid-derived appendages have been prepared and tested as anticancer drugs.[14]

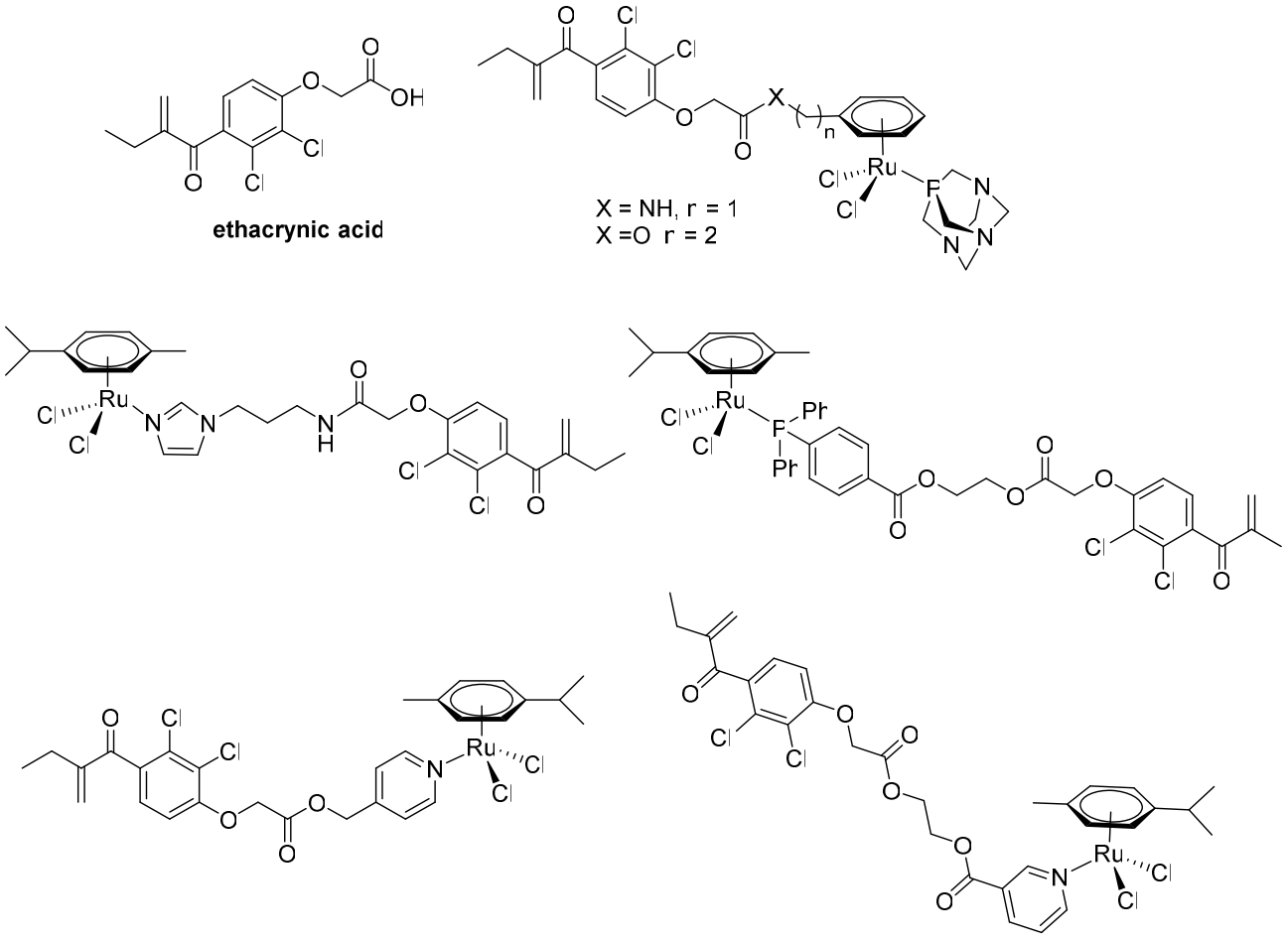

Figure 1. Structures of ethacrynic acid and of arene ruthenium(II) complexes containing ethacrynic acid-modified ligands.

All the ruthenium and platinum complexes modified with ethacrynic acid manifest increased ability to inactivate GSTs and induce apoptosis, even in cisplatin resistant cell lines.[15] To the best of our

knowledge, the inclusion of ethacrynic acid in osmium complexes has not been reported heretofore. In the present paper, the synthesis, characterization and biological activity of a series of four osmium complexes containing ethacrynic acid-modified ligands (including two complexes for which Ru-analogues are known) are described.

Results and discussion

The direct reaction of the bis-acetylacetonato complex Os(η^6-*p*-cymene)(κ*(C)*-acac)(κ*(O,O')*-acac)[16] with ethacrynic acid proceeded at room temperature to give complex **1**, which was isolated as a bright yellow solid in 75% yield (Scheme 1).

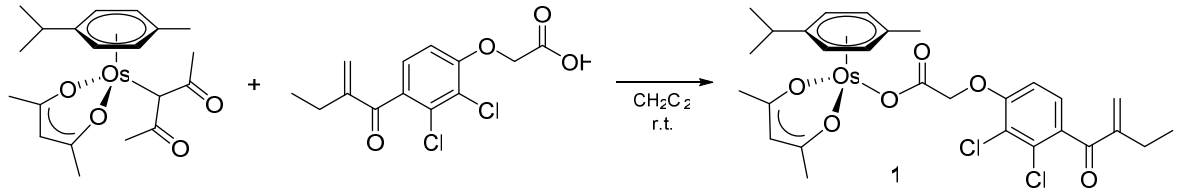

Scheme 1. Synthesis of osmium(II)-*p*-cymene ethacrynato complex **1**.

The ethacrynic acid-functionalized ligands 2-((4-(diphenylphosphanyl)benzyl)oxy)ethyl-2-(2,3-dichloro-4-(2-methylenebutanoyl)phenoxy)acetato (**LP**)[13] and 2-(2-(2,3-dichloro-4-(2-methylenebutanoyl)phenoxy)acetoxy)ethyl-nicotinato (**LN**),[13] and 1,3,5-triaza-7-phosphatricyclo[3.3.1.1]decane (**PTA**)[17] were prepared according to literature procedures. Then the ligands were allowed to react with the dimer [Os(η^6-*p*-cymene)Cl_2]$_2$, to give the corresponding mononuclear complexes **2** and **3** in 90% and 75% yield, respectively, and [Os(η^6-*p*-cymene)Cl_2(**PTA**)][18] (Scheme 2). [Os(η^6-*p*-cymene)Cl_2(**PTA**)]was further treated with **LN**, in the presence of silver tetrafluoroborate, to afford **4** in an overall yield of 81%.

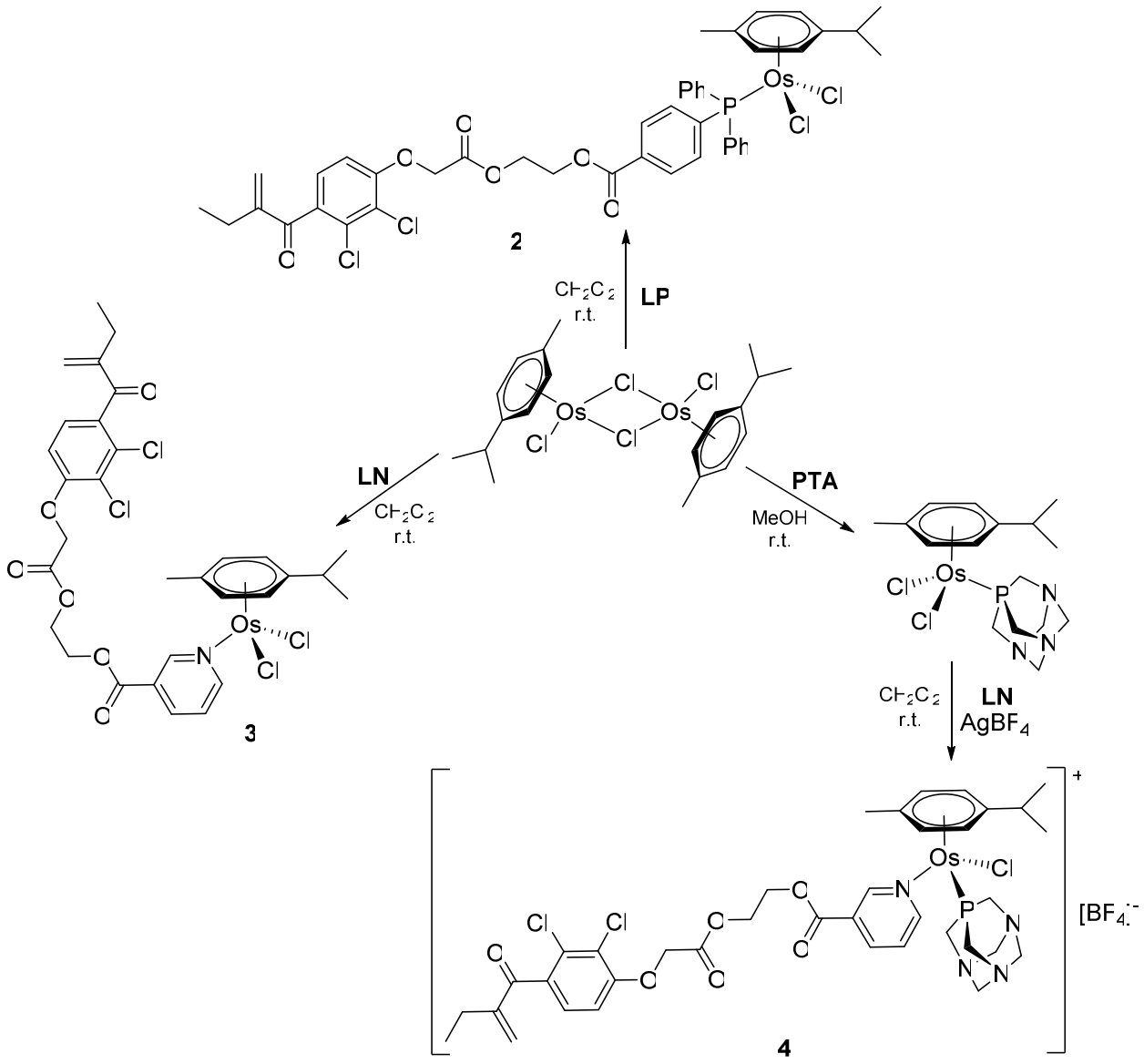

Scheme 2. Synthesis of the complexes **2** – **4** containing ethacrynic acid-modified ligands.

Complexes **1 - 4** are air-stable in the solid state and when dissolved in chlorinated solvents. Complex **4** is a racemate, due to the presence of a stereogenic osmium center. Complexes **1 - 3** in CH_2Cl_2 exhibit molar conductance values in the range 0.12 – 0.41 $S \cdot cm^2 \cdot mol^{-1}$, while the value found for **4** is 9.32 $S \cdot cm^2 \cdot mol^{-1}$, in agreement with the neutral character of **1 - 3** and the ionic character of **4**. The IR spectra of **1 - 4** (solid state) display a series of absorptions in the range 1759-1518 cm^{-1}, attributable to the stretching vibrations of different carbonyl moieties. The NMR spectra of **1-4** (in CD_2Cl_2) contain single sets of resonances. The carbonyl carbon atom of the ethacrynato moiety in **1** exhibits a resonance

at 172.5 ppm in the ^{13}C NMR spectrum, i.e. at comparable frequency than that in ethacrynic acid itself (172.8 ppm). The ^{1}H and ^{13}C NMR spectra of **2 - 3** display the resonances due to the **LP** and **LN** ligands close in value to those observed for the same ligands coordinated in analogous ruthenium complexes.[13] As a consequence of the formal substitution of a chloride with **PTA** on going from the neutral complex **3** to the cationic **4**, the resonances of some pyridyl nuclei undergo significant shift to higher frequency ($\Delta\delta_{C20\text{-}H}$ = 0.27 ppm in the ^{1}H spectra; $\Delta\delta_{C19}$ = 3.1 ppm, $\Delta\delta_{C17}$ = 1.6 ppm and $\Delta\delta_{C20}$ = 2.6 ppm in the ^{13}C spectra; see Chart 4). The ^{31}P NMR resonance in **2** (at −12.1 ppm) appears at lower frequency respect to the free ligand, **LP** (−4.9 ppm),[13] whereas the ^{31}P NMR resonance due to the PTA ligand in **4** (−77.4 ppm) resembles the values previously reported for related arene osmium(II) complexes.[19] The expected structures of **1 - 4** were further corroborated by mass spectrometry and elemental analysis (see Experimental).

Crystals of **1** and **3** suitable for X-ray diffraction analysis were obtained from CH_2Cl_2/pentane and CH_2Cl_2/hexane mixtures, respectively. A small amount of hydroquinone was added in order to facilitate the crystallization of **3**.[20] The structures of **1** and **3** are shown, respectively, in Figures 2 and 3, while selected bond distances and angles are given in Tables 1 and 2. Complexes **1** and **3** adopt the characteristic three-leg piano-stool geometry, comprising the *p*-cymene "seat".[3b,7,18,21] The three "leg" positions are occupied by the bidentate acac ligand [O(5)-Os-O(6) bite angle 88.14(9)º] and the monodentate carboxylate [O(1)-Os-O(5) and O(1)-Os-O(6) angles are 80.59(10)º and 77.35(10)º, respectively] in **1**, and by **LN** and two chlorides in **3** [N(1)-Os-Cl(1), N(1)-Os-Cl(2), and Cl(1)-Os-Cl(2) angles measure 82.20(10)º, 86.62(10)º, and 85.08(4)º, respectively]. The bonding parameters of the EA units are not significantly different from those found in other reported structures.[10a,12,13,22] Compound **1** represents the first example of crystallographically characterized osmium *p*-cymene complex with a monodentate carboxylate ligand: the Os-O(1) bond length [2.081(3) Å] is reminiscent of the situation found in other Os(II)-monodentate carboxylate systems.[23] The Os-O(5) and Os-O(6) bond lengths [2.072(2) and 2.081(2) Å, respectively] in **1** resemble those previously reported for other Os(II)-acac complexes.[21b,24]

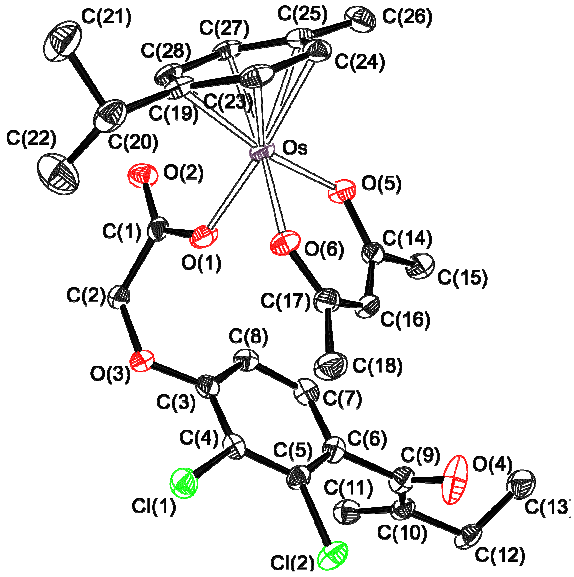

Figure 2. Molecular structure of **1**. Displacement ellipsoids are at the 50% probability level. Hydrogen atoms are omitted for clarity.

Table 1. Selected bond distances (Å) and angles (°) for **1.**

Os-C(23)	2.147(3)	Os-C(24)	2.179(4)
Os-C(25)	2.195(4)	Os-C(27)	2.176(3)
Os-C(28)	2.150(3)	Os-C(19)	2.188(3)
Os-O(5)	2.072(2)	Os-O(6)	2.081(2)
Os-O(1)	2.081(3)	O(1)-C(1)	1.286(4)
O(2)-C(1)	1.224(4)	C(1)-C(2)	1.521(5)
O(5)-Os-O(6)	88.14(9)	O(5)-Os-O(1)	80.59(10)
O(1)-Os-O(6)	77.35(10)	Os-O(1)-C(1)	126.5(2)
O(1)-C(1)-O(2)	128.1(3)	O(1)-C(1)-C(2)	114.0(3)

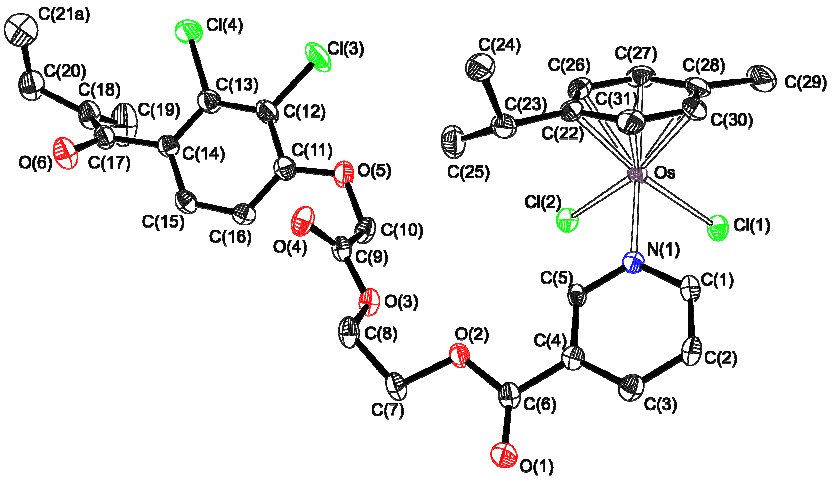

Figure 3. Molecular structure of **3**. Displacement ellipsoids are at the 50% probability level. Hydrogen atoms are omitted for clarity.

Table 2. Selected bond distances (Å) and angles (°) for **3**.

Os-C(22)	2.193(4)	Os-C(26)	2.162(4)
Os-C(27)	2.182(5)	Os-C(28)	2.192(4)
Os-C(30)	2.180(5)	Os-C(31)	2.149(4)
Os-Cl(1)	2.4231(11)	Os-Cl(2)	2.4155(11)
Os-N(1)	2.119(3)	N(1)-Os-Cl(2)	86.62(10)
N(1)-Os-Cl(1)	82.20(10)	Cl(2))-Os-Cl(1)	85.08(4)

NMR and UV-Vis spectroscopy, and conductivity measurements were used to assess the stability of the complexes **1 - 4** in dmso/water solutions at 37 °C as a function of time. Parallel NMR and UV-Vis analyses were carried out also on **1 - 4** in 0.1 M sodium chloride dmso/water solutions (this chloride concentration being similar to that present in blood). The compounds identified from these studies are depicted in Scheme 3.

A complicated mixture of compounds form from **1** in dmso/water, and two sets of resonances have been tentatively assigned to **1a** and **1b**; the ethacrynato moiety behaves as a leaving group, and the NaCl environment accelerates this dissociation. EA-CO_2K was prepared from EA-CO_2H/KN($SiMe_3$)$_2$ and characterized in order to identify EA-CO_2^- in the studied solutions (see Experimental).

Conductivity data suggest that **2 - 4** undergo rapid solvolysis in dmso/water, presumably via the release of a chloride ligand. According to NMR and UV-Vis spectroscopy, this phenomenon does not appear to be inhibited in the presence of NaCl 0.1 M.

It should be noted that the ligands **LP** and **LN** in **2** and **3** are less prone to dissociation than that previously observed for the analogous ruthenium complexes.[13] Indeed, **LP** in **2** is substantially inert towards dissociation (5% released after 72 hours in dmso/water and 12% released after 72 hours in the chloride containing solution). Spectroscopic and conductivity studies indicate that only minor amounts of **3** and **4** remain unchanged in the dmso/water and dmso/water/NaCl solutions for 62-72 hours, and that the **LN** ligand and chloride ligand compete for the exchange with the solvent in both cases. Interestingly, the dissociation of the **LN** ligand from **3** and to a greater extent from **4** is partially suppressed in the respective NaCl solutions.

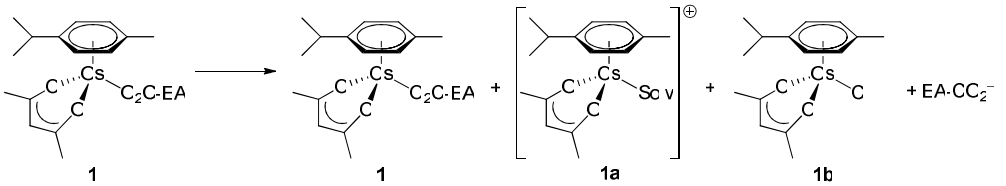

	1	1	1a	1b	
[dmso/H_2C (9 ´ v v), 1 = 72h]		30%	35%	0%	35%
[dmso/H_2C (9 ´ v v)/NaC 1 = 72h]		0%	0%	35%	65%

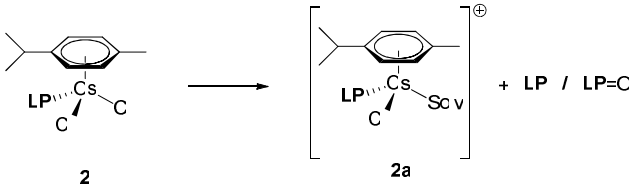

	2	2a		
[dmso/H_2C (9 ´ v v), 1 = 72h]		94%	0%	6%
[dmso/H_2C (9 ´ v v)/NaC 1 = 72h]		88%	7%	5%

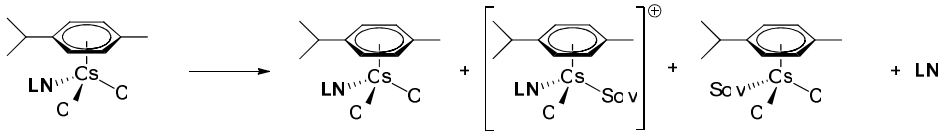

	3	3	3a	3b	
[dmso/H_2C (9 ´ v v), 1 = ´´4h]		6%	3%	46%	45%
[dmso/H_2C (7 3 v v)/NaC 1 = 72h]		´6%	6%	42%	36%

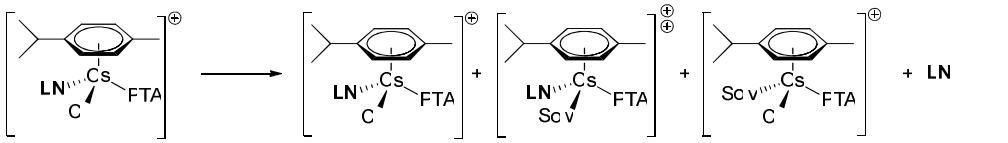

	4	4	4a	4b	
[dmso/H_2C (9 ´ v v), 1 = 62h]		0%	´´%	44%	45%
[dmso/H_2C (´ ´ v v)/NaC 1 = 62h]		9%	45%	46%	not detected [a]

Scheme 3. Compounds detected in dmso/H_2O and dmso/H_2O/NaCl solutions of **1-4** maintained at 37 ℃; % values are based on ^{1}H NMR spectroscopy and refer to the identified compounds only. [a] Not soluble under the experimental conditions.

Cytotoxicity studies

The ability of the complexes **1** – **4** to inhibit cell growth was evaluated against the cisplatin sensitive A2780 and the cisplatin resistant A2780cisR human ovarian carcinoma cell lines and non-tumoral immortalized human embryonic kidney HEK-293 cells (Table 3). All the complexes are considerably more cytotoxic than RAPTA-C on the two cancer cell lines.

Since both EA-CO_2H and EA-(C=O)O$(CH_2)_2$OH might be generated from the ligands/complexes, their antiproliferative activities were also evaluated. The ester EA-(C=O)O$(CH_2)_2$OH shows a 15-20-fold higher cytotoxicity than the carboxylic acid EA-CO_2H, most probably derived from the better uptake of the former into cells, due to increased solubility in the cell culture medium.[10b] Complex **1** has IC_{50} values similar to those determined for EA-CO_2H, whereas **2** - **4** are significantly more cytotoxic, albeit not too dissimilar from their corresponding ethacrynic acid-derived ligands **LP** and **LN**. Complex **3** is more cytotoxic than **4**, both containing the same **LN** ligand, but the latter a **PTA** ligand in place of a chloride ligand. The IC_{50} values of **2** and **3** are comparable to those previously described for ruthenium(II)−arene complexes modified with an ethacrynic acid unit.[10a,12,13] Nonetheless, **2** and **3** display a slightly high selectivity towards cancer cells with respect to non-tumorigenic HEK-293 cells than the respective Ru-analogues (Table 3).[13]

Table 3. IC_{50} values (μM) determined for RAPTA-C,[25] ethacrynic acid (EA-CO_2H),[13] EA-(C=O)O$(CH_2)_2$OH, cisplatin, **LP**,[13] **LN**[13] and **1** - **4** on human ovarian (A2780 and A2780cisR) cancer cells and human embryonic kidney (HEK-293) cells after incubation for 72 h. Values are given as the mean ± SD. Values of the corresponding ruthenium analogues of **2** and **3** are given in parentheses.[13]

	A2780	**A2780cisR**	**HEK-293**
RAPTA-C	230	270	>1000
EA-CO_2H	40 ± 3	53 ± 5	-
EA-(C=O)O$(CH_2)_2$OH	2.0 ± 0.1	3.8 ± 0.7	3.3 ± 0.5
LP	9 ± 1	40 ± 4	38 ± 9

LN	13 ± 2	11 ± 1	7 ± 1
1	43 ± 6	69 ± 2	40 ± 4
2	13 ± 2	20 ± 5	21 ± 2
	(11 ± 2)	(15 ± 4)	(13 ± 4)
3	8 ± 1	26 ± 8	13 ± 1
	(13 ± 3)	(26 ± 2)	(16 ± 3)
4	17 ± 3	34 ± 1	25 ± 2
cisplatin	0.9 ± 0.1	25 ± 3	9 ± 2

Intracellular GST inhibition

Due to the potential of **1 - 4** to inhibit GSTs inside cells, residual intracellular GST activity after incubation with the complexes and the ligands at the respective IC_{50} concentrations was determined by fluorescence spectroscopy in A2780 and A2780cisR cells (Figure 4). Incubation for 18 hours led to a modest decrease in GST activity in both A2780 and A2780cisR cells with all the compounds, **1** being the least effective GST inhibitor. This appears to be in accordance with the low cytotoxicity exhibited by **1**, which is prone to quickly release the ethacrynato anion in aqueous conditions (see above).

In principle, both the EA-CO_2H and EA-$(C{=}O)O(CH_2)_2OH$ fragments might be generated inside the cells following dissociation of **LN** and **LP** from **2 - 4**.[15,26] The most pronounced effects on GST activity were observed for **2** (20% inhibition) and **4** (30% inhibition) in A2780 cells and to a lesser extent in A2780cisR cells, which indicates that the GSH/GST detoxification system in A2780cisR cells is more active, reflected by twofold higher IC_{50} values, compared to A2780 cells (Table 3).

The ligand **LN** inhibits GST in A2780cisR cells slightly more than in A2780 cells, which might contribute to the comparable cytotoxicity in A2780 cells and A2780cisR cells, respectively (Table 3). The intracellular GST inhibition values of **2 - 4** do not correlate directly with the IC_{50} values (compare Table 3 and Figure 4), thus suggesting that the cytotoxicity of the compounds may only be partially attributed to GST inhibition. Indeed, these results are consistent with a previous mechanistic study on a bifunctional arene ruthenium(II)-ethacrynic acid compound, indicating that the EA-unit inhibits GSTs, releasing the organometallic fragment which leads to a surge of cell death.[15a]

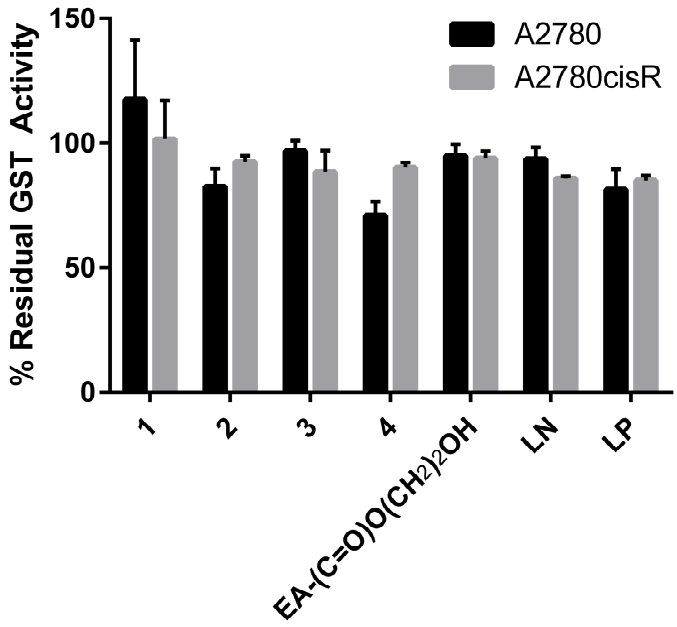

Figure 4. Residual GST activity in A2780 and A2780cisR cells, expressed as % activity of control, after incubation at IC_{50} concentrations for 18 h. The changes in fluorescence over a 20 min period were used to calculate GST activities.

Conclusions

The first osmium complexes containing ethacrynic acid, a broad acting inhibitor of GSTs, have been synthesized and characterized. For two of the complexes, **2** and **3**, ruthenium analogues are known, whereas **1** and **4** are unique in that no ruthenium congeners have been reported. Compounds **2** and **3** are, as expected, more stable than the ruthenium analogues, in dmso/water and dmso/water/NaCl solutions. To within experimental error, there is no significant trend indicating that complexes of one metal (Ru or Os) are substantially more cytotoxic than the analogues of the other one, as previously noted.[27] The complex with the most stable Os-EA ligand bond, i.e. **2**, in which the ethacrynic acid entity is connected to the osmium(II) ion via a P-donor ligand, is not the most cytotoxic compound, indicating that dissociation of the bioactive EA group from the metal ion could be important in the mechanism of drug action. Indeed, the antiproliferative activity of **2** may be attributed predominantly to the ethacrynic acid-derived ligand, as their IC_{50} values are similar. This could explain why there is not a direct correlation between cytotoxicity and inhibition of intracellular GSTs, as the data suggest that GSTs are relevant targets, but not exclusive targets. Finally, incorporation of the pta ligand in **3** to

afford **4** does not improve the cytotoxicity or selectivity of the compounds, presumably due to the major role of the ethacrynic acid-derived ligand in the overall biological activity observed.

Experimental

$OsCl_3 \cdot 3H_2O$ (54% purity approx.) was purchased from Heraeus, while the organic reactants were purchased from Acros Organics and were of the highest purity available. Solvents were purchased from Scharlau and then obtained oxygen- and water-free with a MBraun solvent purification apparatus. The ligands **PTA**,[17] **LP** [13] and **LN** [13] and the complexes $[(\eta^6\text{-}p\text{-cymene})OsCl_2]_2$,[28] Os($\eta^6$-*p*-cymene)($\kappa$*(C)*-acac)($\kappa$*(O,O')*-acac) [16] and Os(η^6-*p*-cymene)Cl_2(**PTA**) [18] were prepared according to the respective literature methods. NMR spectra were recorded on either a Bruker ARX 300 MHz or a Bruker Avance 300 MHz instrument. Chemical shifts (expressed in parts per million) are referenced to the residual solvent peaks (^{1}H, ^{13}C{^{1}H}) or to external standard (^{31}P{^{1}H} to 85% H_3PO_4). Coupling constants are given in Hz. Conductivity measurements were carried out using an Eutech Con 700 instrument (cell constant = 1.0 cm^{-1}).[29] UV-vis spectra were recorded with an Ultraspec 2100 Pro spectrophotometer. Attenuated total reflection infrared spectra (ATR-IR) of solid samples were recorded on a Perkin-Elmer Spectrum 100 FT-IR spectrometer. C, H, and N analyses were carried out with a Perkin-Elmer 2400 CHNS/O analyzer. High-resolution electrospray mass spectra (HRMS) were acquired using a MicroTOF-Q hybrid quadrupole time-of-flight spectrometer (Bruker Daltonics, Bremen, Germany).

Synthesis of Os(η^6-*p*-cymene)(acetylacetonato)(2-(2,3-dichloro-4-(2-ethylenebutanoyl)phenoxy) acetato), 1

A solution of Os(η^6-*p*-cymene)(κ*(C)*-acac)(κ*(O,O')*-acac) (0.097 g, 0.19 mmol) in CH_2Cl_2 (5 mL) was treated with EA-CO_2H (0.069 g, 0.23 mmol) and then left stirring at room temperature for 24 hours. The solvent was removed under vacuo to obtain a red oily residue. Repeated washings with Et_2O (3 x 10 mL) afforded **1** as a bright yellow powder. Yield 0.103 g, 75%. Crystals suitable for X-ray analysis were obtained by slow diffusion of pentane into a CH_2Cl_2 solution of **1**. Anal. calcd. for $C_{28}H_{32}Cl_2O_6Os$: C, 46.34; H, 4.44. Found: C, 46.34; H, 4.28. ESI-MS(+): *m/z* found 749.106 $[M+Na]^+$, calcd. for $C_{28}H_{32}Cl_2NaO_6Os^+$ 749.108; the isotopic pattern fits well the calculated one. IR (solid state) υ: 2966w, 2936w, 2912w, 2876w, 1660m, 1644s, 1587m, 1575m, 1556m, 1518s, 1469m, 1434w, 1383m, 1358vs, 1343w, 1285m, 1270m, 1265s, 1244w, 1219w, 1197w, 1146w, 1120w, 1083w, 1060s, 1031w, 1006m, 962w, 938w, 925w, 891w, 864m, 823w, 803s, 785m, 757w, 729s, 684w, 659w, 633m,

610m cm^{-1}. UV-Vis (CH_2Cl_2): λ_{max}/nm ($\varepsilon/M^{-1}cm^{-1}$) = 263 ($7.4\cdot10^3$), 327 ($1.9\cdot10^3$). Λ_M (CH_2Cl_2) = 0.12 $S\cdot cm^2\cdot mol^{-1}$. ^1H NMR (CD_2Cl_2): δ = 7.01 (d, 1H, $^3J_{HH}$ = 8.6 Hz, C11-H); 6.59 (d, 1H, $^3J_{HH}$ = 8.6 Hz, C10-H); 6.06, 5.82 (d, 4H, $^3J_{HH}$ = 5.6 Hz, arom CH_{cymene}); 5.91, 5.58 (m, 2H, C4-H); 5.04 (s, 1H, CH_{acac}); 4.55 (s, 2H, C12-H); 2.64 (sept, 1H, $^3J_{HH}$ = 6.9 Hz, CHMe$_2$); 2.43 (q, 2H, $^3J_{HH}$ = 7.4 Hz, C2-H); 2.17 (s, 3H, *Me*C_6H_4); 1.80 (s, 6H, Me_{acac}); 1.24 (d, 6H, $^3J_{HH}$ = 6.9 Hz, CH*Me*$_2$); 1.12 ppm (t, 3H, $^3J_{HH}$ = 7.4 Hz, C1-H). $^{13}C\{^1H\}$ NMR (CD_2Cl_2): δ = 196.3 (C5); 185.8 (*C*O_{acac}); 172.5 (C13); 157.0 (C9); 150.8 (C3); 132.5 (C8); 131.0 (C7); 128.3 (C4); 127.3 (C11); 122.3 (C6); 110.6 (C10); 99.2 (*C*H_{acac}); 88.6 (*C*CHMe$_2$); 88.0 (*C*Me_{cymene}); 73.2, 68.5 (arom *C*H_{cymene}); 67.7 (C12); 32.0 (*C*HMe$_2$); 27.0 (Me_{acac}); 24.1 (C2); 22.9 (CH*Me*$_2$); 18.4 (*Me*C_6H_4); 12.8 ppm (C1).

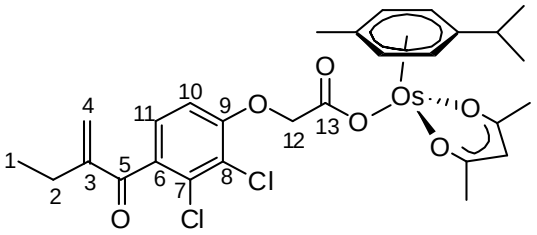

Chart 1. Os(η^6-*p*-cymene)(κ*(O,O')*-acac)(κ*(O)*-O_2C-EA), **1** (numbering refers to carbon atoms).

Synthesis of Os(η^6-*p*-cymene)Cl_2(2-((4-(diphenylphosphanyl)benzyl)oxy)ethyl-2-(2,3-dichloro-4-(2-methylenebutanoyl)phenoxy)acetato), 2

Compound [Os(η^6-*p*-cymene)Cl_2]$_2$ (0.137 g, 0.173 mmol) was added to a solution of **LP** (0.265 g, 0.417 mmol) in CH_2Cl_2 (10 mL). The resulting orange solution was left stirring for 3 h at room temperature, then the volatile substances were removed under vacuo to afford an orange foamy residue. This solid was dissolved into a small volume of CH_2Cl_2 and loaded on top of a silica column (h 4.5 cm, d 2.5 cm). Impurities were eluted with CH_2Cl_2, then an orange band was eluted with CH_2Cl_2:THF 1:1 *v*/*v*. Complex **2** was finally obtained as an orange powder after solvent removal under vacuo (50°C). Yield 0.319 g (90%). Anal. calcd. for $C_{44}H_{43}Cl_4O_6OsP$: C, 51.27; H, 4.20. Found: C, 51.08; H, 4.33. ESI-MS(+): *m/z* found 1053.097 $[M+Na]^+$, calcd. for $C_{44}H_{43}Cl_4NaO_6OsP^+$ 1053.105; the isotopic pattern fits well the calculated one. IR (solid state) *υ*: 3058w, 2963w, 2957w, 1759m, 1720s, 1662m, 1584m, 1568w, 1468m, 1435m, 1391w, 1384m, 1339w, 1263s, 1187s, 1111m, 1079vs, 1030m, 1017m, 1000m, 948w, 895w, 858w, 800m, 762m, 749m, 721m, 696vs, 632w, 565w, 541s, 519vs cm^{-1}. UV-Vis (CH_2Cl_2): λ_{max}/nm ($\varepsilon/M^{-1}cm^{-1}$) = 250 ($2.3\cdot10^4$), 322 ($1.9\cdot10^3$). Λ_M (CH_2Cl_2) = 0.25 $S\cdot cm^2\cdot mol^{-1}$. ^1H NMR (CD_2Cl_2): δ = 7.91-7.73, 7.44 (14H, C18-H + C18'-H + C19-H + C19'-H + Ph); 7.13 (d, 1H, $^3J_{HH}$ = 8.5 Hz, C11-H), 6.84 (d, 1H, $^3J_{HH}$ = 8.5 Hz, C10-H); 5.95, 5.58 (m, 2H, C4-H); 5.43, 5.19 (d, 4H,

$^3J_{HH}$ = 5.6 Hz, arom CH_{cymene}); 4.80 (s, 2H, C12-H); 4.54 (s, 4H, C14-H + C15-H); 2.69 (sept, 1H, $^3J_{HH}$ = 6.9 Hz, CHMe$_2$); 2.45 (q, 2H, $^3J_{HH}$ = 7.4 Hz, C2-H); 1.98 (s, 3H, *Me*C$_6$H$_4$); 1.17 (d, 6H, $^3J_{HH}$ = 6.8 Hz, CH*Me*$_2$); 1.14 ppm (t, 3H, $^3J_{HH}$ = 7.2 Hz, C1-H). $^{13}C\{^1H\}$ NMR (CD_2Cl_2): δ = 196.3 (C5); 168.4 (C13); 166.4 (C16); 156.1 (C9); 151.0 (C3); 140.7, 140.1 (m, C20 + P-*C*); 135.5-135.3 (m, C19 + C19' + arom *C*H$_{Ph}$); 134.0 (C8); 133.4 (C7); 131.4 (C17); 131.3 (arom *C*H$_{Ph}$); 129.4 (C4); 129.2, 128.9 (m, C18 + C18' + arom *C*H$_{Ph}$); 127.7 (C11); 123.7 (C6); 111.7 (C10); 103.9 (*C*CHMe$_2$); 90.0 (arom *C*Me); 81.4 (d, $^2J_{PC}$ = 2.8 Hz, arom *C*H$_{cymene}$); 81.1 (d, $^2J_{PC}$ = 4.6 Hz, arom *C*H$_{cymene}$); 66.9 (C12); 64.1, 63.3 (C14 + C15); 31.0 (*C*HMe$_2$); 24.2 (C2); 22.8 (CH*Me*$_2$); 18.4 (*Me*C$_6$H$_4$); 13.0 ppm (C1). ^{31}P NMR (CD_2Cl_2): δ = −12.1 ppm.

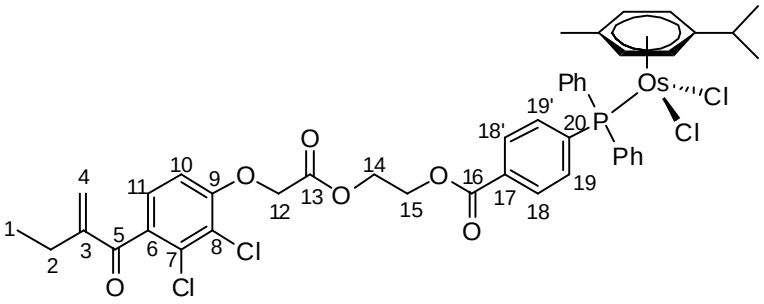

Chart 2. Os(η^6-*p*-cymene)Cl$_2$(**LP**), **2** (numbering refers to carbon atoms).

Synthesis of Os(*η*^{6}-*p*-cymene)Cl$_2$(2-(2-(2,3-dichloro-4-(2-methylenebutanoyl)phenoxy)acetoxy) ethyl nicotinato), 3

This compound was prepared by the same procedure described for the synthesis of **2**, from [(η^6-*p*-cymene)OsCl$_2$]$_2$ (0.100 g, 0.126 mmol) and **LN** (0.139 g, 0.307 mmol). Yellow solid, yield 0.153 g (75%). Crystals of **3**·CH$_2$Cl$_2$·½[1,4-C$_6$H$_4$(OH)$_2$] suitable for X-ray analysis were obtained by slow diffusion of hexane into a CH$_2$Cl$_2$ solution of **3**, added of a few grains of hydroquinone. Anal. calcd. for $C_{31}H_{33}Cl_4NO_6Os$: C, 43.93; H, 3.92; N, 1.65. Found: C, 44.25; H, 4.10; N, 1.62. ESI-MS(+): *m/z* found 812.096 $[M\text{-}Cl]^+$, calcd. for $C_{31}H_{33}Cl_3NO_6Os^+$ 812.099; the isotopic pattern fits well the calculated one. IR (solid state) *υ*: 2964w, 2940w, 2893w, 1751m, 1728s, 1662m, 1584m, 1467w, 1432w, 1383w, 1339w, 1286vs, 1194vs, 1137s, 1116s, 1079vs, 1062s, 1025m, 1000m, 941w, 891w, 876w, 820w, 803m, 767w, 745s, 702w, 689m, 637w cm^{-1}. UV-Vis (CH$_2$Cl$_2$): λ_{max}/nm (ε/M^{-1}cm^{-1}) = 259 (1.0·10^4), 282 (6.8·10^3), 322 (4.3·10^3). Λ_M (CH$_2$Cl$_2$) = 0.41 S·cm^2·mol^{-1}. ^1H NMR (CD_2Cl_2): δ = 9.51 (s, 1H, C18-H); 9.13 (m, 1H, C19-H); 8.29 (m, 1H, C21-H); 7.47 (m, 1H, C20-H); 7.18 (d, 1H, $^3J_{HH}$ = 8.6 Hz, C11-H); 6.95 (d, 1H, $^3J_{HH}$ = 8.6 Hz, C10-H); 5.99, 5.61 (m, 2H, C4-H); 5.86, 5.64 (d, 4H, $^3J_{HH}$ = 5.7 Hz, arom CH_{cymene}); 4.94 (s, 2H, C12-H); 4.62 (s, 4H, C14 + C15); 2.80 (sept, 1H, $^3J_{HH}$ = 6.9 Hz,

C*H*Me$_2$); 2.47 (q, 2H, $^3J_{HH}$ = 7.4 Hz, C2-H); 2.03 (s, 3H, *Me*C$_6$H$_4$); 1.31 (d, 6H, $^3J_{HH}$ = 6.9 Hz, CH*Me*$_2$); 1.16 ppm (t, 3H, $^3J_{HH}$ = 7.4 Hz, C1-H). $^{13}C\{^1H\}$ NMR (CD_2Cl_2): δ = 196.0 (C5); 168.3 (C13); 163.7 (C16); 158.1 (C19); 155.9 (C18); 155.8 (C9); 150.7 (C3); 139.1 (C21); 134.3 (C8); 131.6 (C7); 129.1 (C4); 127.6 (C11); 127.4 (C17); 125.0 (C20); 123.3 (C6); 111.5 (C10); 94.1 (*C*CHMe$_2$); 89.4 (arom *C*Me); 75.9, 73.4 (arom *C*H$_{cymene}$); 66.6 (C12); 63.9, 63.3 (C14, C15); 31.5 (*C*HMe$_2$); 23.9 (C2); 22.8 (CH*Me*$_2$); 18.4 (*Me*C$_6$H$_4$); 12.8 ppm (C1).

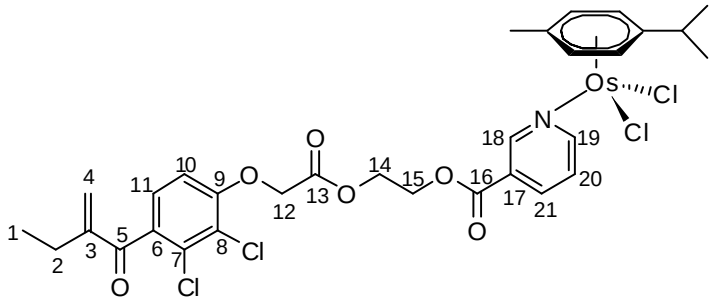

Chart 3. (η^6-*p*-cymene)OsCl$_2$(**LN**), **3** (numbering refers to carbon atoms).

Synthesis of Os(*η*^{6}-*p*-cymene)Cl(2-(2-(2,3-dichloro-4-(2-methylenebutanoyl)phenoxy)acetoxy) ethylnicotinato)(1,3,5-triaza-7-phosphaadamantane) tetrafluoroborato, 4

A stirred solution of Os(*η*^{6}-*p*-cymene)Cl$_2$(**PTA**) (0.100 g, 0.181 mmol) in CH_2Cl_2 (6 mL) was treated with **LN** (0.098 g, 0.216 mmol) and then with $AgBF_4$ (0.048 g, 0.25 mmol). The mixture was stirred for 72 h at room temperature under protection from the light. The final mixture was filtered through Celite, then the volatiles substances were removed under vacuo. The residue was precipitated with Et_2O (30 mL) and then washed with hexane (20 mL). Complex **4** was obtained as a pale-yellow solid. Yield 0.156 g (81%). Anal. calcd. for $C_{37}H_{45}BCl_3F_4N_4O_6OsP$: C, 42.08; H, 4.29; N, 5.30. Found: C, 42.70; H, 4.36; N, 5.47. ESI-MS(+): *m/z* found 969.177 $[M]^+$, calcd. for $C_{37}H_{45}Cl_3N_4O_6OsP^+$ 969.175; the isotopic pattern fits well the calculated one. IR (solid state) *υ*: 2967w, 2936w, 2880w, 1757m-sh, 1733s, 1662m, 1585m, 1469m, 1444w-m, 1385w-m, 1288s, 1242m, 1197s, 1138m, 1117s-sh, 1054vs-br, 973s, 947s, 896m, 803m, 766w-m, 744s, 695w-m, 606w, 577s cm^{-1}. UV-Vis (CH_2Cl_2): λ_{max}/nm (ε/M^{-1}cm^{-1}) = 258 ($1.4\cdot10^4$), 317 ($5.2\cdot10^3$). Λ_M (CH_2Cl_2) = 9.32 S·cm^2·mol^{-1}. ^1H NMR (CD_2Cl_2): δ = 9.55 (s, 1H, C18-H); 9.09 (d, 1H, $^3J_{HH}$ = 5.5 Hz, C19-H); 8.43 (d, 1H, $^3J_{HH}$ = 8.0 Hz, C21-H); 7.74 (m, 1H, C20-H); 7.15 (d, 1H, $^3J_{HH}$ = 8.6 Hz, C11-H); 6.89 (d, 1H, $^3J_{HH}$ = 8.6 Hz, C10-H); 6.03, 5.79 (d, 4H, $^3J_{HH}$ = 5.7 Hz, arom C*H*$_{cymene}$); 5.96, 5.58 (m, 2H, C4-H); 4.88 (d, 2H, $^2J_{HH}$ = 1.5 Hz C12-H); 4.71-4.58 (m, 6H, NCH$_2$N); 4.62 (s, 4H, C14 + C15); 4.19 (q, 6H, $^2J_{HP}$ = 15.4 Hz, NCH$_2$P); 2.54 (sept, 1H, $^3J_{HH}$ = 6.6 Hz, C*H*Me$_2$); 2.44 (q, 2H, $^3J_{HH}$ = 7.3 Hz, C2-H); 2.05 (s, 3H, *Me*C$_6$H$_4$); 1.26 (d, 6H, $^3J_{HH}$ = 6.8 Hz, CH*Me*$_2$); 1.13 ppm (t, 3H, $^3J_{HH}$ = 7.4 Hz, C1-H). $^{13}C\{^1H\}$ NMR (CD_2Cl_2): δ = 196.1 (C5); 168.4 (C13);

163.2 (C16); 161.2 (C19); 156.7 (C18); 155.9 (C9); 150.8 (C3); 140.8 (C21); 134.6 (C8); 131.8 (C7); 129.2 (C4); 129.0 (C17); 127.6 (C11); 127.6 (C20); 123.3 (C6); 111.7 (C10); 104.3 (*C*CHMe$_2$); 95.0 (arom *C*Me); 75.9, 73.4 (arom *C*H$_{cymene}$); 72.9 (NCH$_2$N); 66.8 (C12); 64.5, 63.5 (C14, C15); 49.5 (d, $^1J_{CP}$ = 21.1 Hz, NCH$_2$P); 31.6 (*C*HMe$_2$); 24.0 (C2); 23.0, 22.4 (CH*Me*$_2$); 18.4 (*Me*C$_6$H$_4$); 12.8 ppm (C1). ^{31}P NMR (CD_2Cl_2): δ = –77.4 ppm.

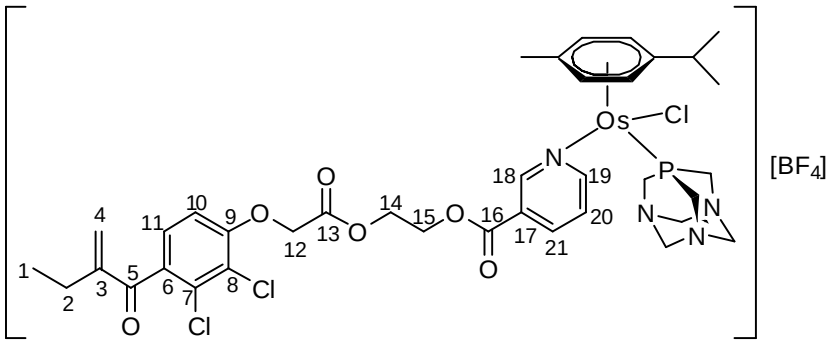

Chart 4. [(η^6-*p*-cymene)OsCl(**LN**)(**PTA**)][BF$_4$], **4** (numbering refers to carbon atoms).

Synthesis of EA-CO$_2$K. KN(SiMe$_3$)$_2$ (0.36 mL, 0.33 mmol) was added to a solution of EA-CO$_2$H (0.100 g, 0.330 mmol) in Et$_2$O (10 mL), under nitrogen atmosphere. The mixture was left stirring for additional 24 h. The resulting colorless solid was separated, washed with pentane (20 mL) and dried under vacuo. Yield 0.075 g, 66.6%. Anal. calcd. for $C_{13}H_{11}Cl_2KO_4$: C, 45.76; H, 3.25; Cl, 20.78. Found: C, 45.71; H, 3.18; Cl, 20.82. IR (solid state): ν = 2965w, 2938w, 2922w, 2878w, 2550w, 1657m (C=O), 1598vs (COO), 1586vs, 1554m, 1471m-s, 1417s, 1385m, 1339m, 1267m-s, 1202m, 1120w, 1054vs, 1002m, 941m, 908w, 824w, 799s, 760m, 737m, 724m, 698w, 680w, 627m, 590w, 570w, 531w cm^{-1}. ^{1}H NMR (D_2O): δ = 7.26 (d, $^3J_{HH}$ = 8.80 Hz, 1H, C10-H); 6.92 (d, $^3J_{HH}$ = 8.80 Hz, 1H, C11-H); 6.08, 5.69 (s, 2 H, C4-H); 4.58 (s, 2 H, C12-H); 2.36 (m, 2 H, C2-H); 1.06 (m, 3 H, C1-H) ppm. ^{13}C NMR (D_2O): δ = 199.2 (C5); 174.9 (C13); 156.1 (C9); 150.1 (C6); 131.8 (C7), 131.6 (C8); 130.3 (C3); 128.0 (C11); 122.0 (C4); 111.1 (C10); 67.8 (C12); 23.2 (C2); 12.0 (C1) ppm.

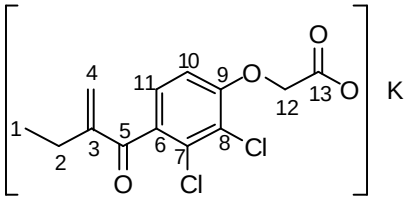

Chart 5. EA-CO$_2$K (numbering refers to carbon atoms).

Stability studies

General procedure. Complexes **1**−**4** were dissolved in the selected d^6-dmso/D_2O mixture (2.0 mL) ([Os] = $2.1\cdot10^{-2}$ mol L^{-1}). An aliquot of the resulting solution (0.40 mL) was transferred into a NMR tube, maintained at 37 °C and analyzed by NMR spectroscopy as a function of time. The remaining solution was diluted up to 4.2 mL with the appropriate dmso/water mixture (final [Os] = $7.8\cdot10^{-3}$ mol L^{-1}), maintained at 37 °C and analyzed by conductivity measurements and UV-Vis spectroscopy as a function of time (t). Parallel analyses were carried out on dmso/water mixtures prepared by the same procedure described above, and with the addition of NaCl (ca. 0.1 M). CH_3OD ($2.5\cdot10^{-2}$ mol L^{-1}) was used as a reference for the ^1H NMR spectra. For NMR assignments refer to Scheme 3. The NMR spectra of **LP**, **LN**, EA-CO_2H, EA-C(=O)O$(CH_2)_2$OH, **PTA** and acacH were recorded in d^6-dmso/D_2O (9:1 *v*/*v*) and used for comparison for NMR assignments. $FeCp_2$ was selected as an organometallic standard for conductivity data (Λ_M = 0.69 $S\cdot cm^2\cdot mol^{-1}$ in dmso/H_2O 9:1 at 37 °C).

Compound **1**. Λ_M (dmso/water 9:1) = 3.4 $S\cdot cm^2\cdot mol^{-1}$ (t = 5 min); 5.3 $S\cdot cm^2\cdot mol^{-1}$ (t = 50 min); 4.6 $S\cdot cm^2\cdot mol^{-1}$ (t = 6 h); 5.3 $S\cdot cm^2\cdot mol^{-1}$ (t = 24 h); 3.8 $S\cdot cm^2\cdot mol^{-1}$ (t = 114 h). UV-Vis (dmso/water 9:1), λ_{max}/nm ($\varepsilon/M^{-1}cm^{-1}$) = 327 ($2.6\cdot10^3$) (t = 2 h - 114 h). UV-Vis (dmso/water 9:1 + NaCl 0.1 M) = 330 ($2.7\cdot10^3$) (t = 2 h); 330 ($2.1\cdot10^3$) (t = 72 h). ^1H NMR (d6-dmso/D_2O 9:1): δ = 7.23 (d, $EACO_2^-$), 7.16 (d, **1**), 6.91 (d, $EACO_2^-$), 6.67 (d, **1**), 6.24 (s, **1a**), 6.13 (s, **1a**), 6.03 (s, **1** + $EACO_2^-$), 5.86 (s, **1a**), 5.55 (s, $EACO_2^-$), 5.54 (s, **1**), 4.97 (s, **1**), 4.52 (s, **1**), 4.47 (s, $EACO_2^-$), 2.33 (q, **1** + $EACO_2^-$), 1.95 (s, **1**), 1.69 (s, **1** + **1a**), 1.20 (d, **1**), 1.14 (d, **1a**), 1.04 (t, **1** + $EACO_2^-$). Ratio **1** : $EACO_2^-$: **1a** = 1:1:1 (t = 1 - 72 h). ^1H NMR (d6-dmso/D_2O 9:1 + NaCl 0.1 M): **1**, $EACO_2^-$ and **1b** [δ = 6.00 (d), 5.78 (d), 5.31 (s), 2.08 (s), 1.80 ppm (s)], ratio 2:8:7 (t = 5 min), 0:5:3 (t = 2 - 72 h).

Compound **2**. Λ_M (dmso/water 9:1) = 8.9 $S\cdot cm^2\cdot mol^{-1}$ (t = 5 min - 72 h). UV-Vis (dmso/water 9:1), λ_{max}/nm ($\varepsilon/M^{-1}cm^{-1}$) = 322 ($2.8\cdot10^3$), 423 ($4.3\cdot10^2$) (t = 5 min - 72 h). UV-Vis (dmso/water 9:1 + NaCl 0.1 M) = 320 ($2.8\cdot10^3$), 423 ($4.0\cdot10^2$) (t = 5 min); 320 ($2.4\cdot10^3$), 423 ($4.0\cdot10^2$) (t = 72 h). ^1H NMR (d6-dmso/D_2O 9:1 or d6-dmso/D_2O 9:1 + NaCl 0.1 M): δ = 7.85 (m, 2H), 7.79 (m, 2H), 7.64 (m, 4H), 7.43 (m, 6H), 7.18, 7.11 (d, 2H), 6.00 (s, 1H), 5.50, 5.37 (d, 4H), 5.47 (s, 1H), 5.01 (s, 2H), 4.45 (s, 4H), 2.41 (m, 1H), 2.31 (q, 2H), 1.83 (s, 3H), 1.02 (t, 3H), 0.98 ppm (d, 6H) (t = 5 min - 72 h). $^{13}C\{^1H\}$ NMR (d6-dmso/D_2O 9:1 or d6-dmso/D_2O 9:1 + NaCl 0.1 M): δ = 195.7, 168.4, 165.7, 155.5, 149.7, 134.8-134.5, 133.3, 133.0, 132.9, 131.1, 130.1, 128.6-128.4, 127.8, 112.1, 88.9, 81.3, 80.3, 66.0, 63.4, 63.2, 30.1, 23.3, 22.1, 17.5, 12.7 ppm (t = 5 min - 72 h). ^{31}P NMR (d6-dmso/D_2O 9:1): δ = –12.8 ppm (t = 5 min - 22 h); δ = –12.8 (major, **2a**), 26.6 (ca. 6%, **LP**=O) ppm (t = 51 h - 72 h). ^{31}P NMR (d6-

dmso/D_2O 9:1 + NaCl 0.1 M): δ = –12.8 (major, **2a**), 26.6 (ca. 9%, **LP**=O) ppm (t = 5 min - 23 h); –12.8 (major, **2a**), –6.3 (**LP,** ca. 7%), 26.6 (ca. 5%, **LP**=O) ppm (t = 72 h).

Compound **3**. Λ_M (dmso/water 9:1) = 2.2 $S \cdot cm^2 \cdot mol^{-1}$ (t = 5 min); 3.2 $S \cdot cm^2 \cdot mol^{-1}$ (t = 50 min); 3.4 $S \cdot cm^2 \cdot mol^{-1}$ (t = 6 h); 3.3 $S \cdot cm^2 \cdot mol^{-1}$ (t = 24 h); 3.9 $S \cdot cm^2 \cdot mol^{-1}$ (t = 114 h). UV-Vis (dmso/water 9:1), λ_{max}/nm ($\varepsilon/M^{-1}cm^{-1}$) = 322 ($2.2 \cdot 10^3$), 418 ($3.6 \cdot 10^2$) (t = 5 min - 72 h). UV-Vis (dmso/water 7:3 + NaCl 0.1 M) = 322 ($1.6 \cdot 10^3$), 418 ($2.4 \cdot 10^2$) (t = 5 min); 322 ($1.8 \cdot 10^3$), 418 ($2.4 \cdot 10^2$) (t = 72 h). ^{1}H NMR (d6-dmso/D_2O 9:1): δ = 9.30 (s, **3** + **3a**), 9.04 (s, **LN**), 8.99 (t, **3a**), 8.98 (d, **3**), 8.78 (d, **LN**), 8.47 (d, **3a**), 8.30 (d, **3**), 8.24 (d, **LN**), 7.77 (m, **3a**), 7.59 (dd, **3**), 7.54 (dd, **LN**), 7.23 (d, **3** + **3a**), 7.16 (d, **LN**), 7.14 (m, **3a**), 7.10 (d, **LN**), 6.38 (d, **3a**), 6.25 (d, **3a**), 6.17 (d, **3a**), 6.08 (d, **3a**), 6.04 (d, **3b**), 6.03 (s, **LN**), 5.94 (d, **3b**), 5.92 (d, **3**), 5.74 (d, **3**), 5.52 (s, **3a**), 5.49 (s, **LN**), 5.04 (s, **LN**), 4.50 (s, **LN**), 2.70 (m, **3b**), 2.33 (q, **LN**), 2.14 (s, **3a**), 2.11 (s, **3b**), 1.89 (s, **3**), 1.17 (d, **3b**), 1.04 ppm (t, **LN**). Ratio **3** : **3a** : **3b** : **LN** = 13:0:87:88 (t = 5 min), 10:7:79:82 (t = 1 h), 10:5:83:87 (t = 3 h), 11:6:82:77 (t = 48 h), 11:6:83:81 (t = 114 h). ^{1}H NMR (d6-dmso/D_2O 7:3 + NaCl 0.1 M): **3**, **3a**, **3b** and **LN**, ratio 25:10:70:60 (t = 5 min - 72 h). $^{13}C\{^1H\}$ NMR (d6-dmso/D_2O 9:1): δ = 195.7 (**LN**), 168.4 (**LN**), 165.1 (**LN**), 155.5 (**LN**), 154.1 (**LN**), 150.4 (**LN**), 149.7 (**LN**), 137.5 (**LN**), 133.0 (**LN**), 130.1 (**LN**), 127.8 (**LN**), 125.8 (**LN**), 124.4 (**LN**), 121.5 (**LN**), 112.0 (**LN**), 98.4 (**3b**), 93.6 (**3b**), 78.5 (**3b**), 78.4 (**3b**), 65.9 (**LN**), 63.5 (**LN**), 63.1 (**LN**), 30.3 (**3b**), 23.3 (**LN**), *)*: 22.1 (**3b**), 18.1 (**3b**), 12.7 ppm (**LN**) (t = 72 h).

Compound **4**. Λ_M (dmso/water 9:1) = 67 $S \cdot cm^2 \cdot mol^{-1}$ (t = 5 min); 60 $S \cdot cm^2 \cdot mol^{-1}$ (t = 2 h); 65 $S \cdot cm^2 \cdot mol^{-1}$ (t = 24 h); 71 $S \cdot cm^2 \cdot mol^{-1}$ (t = 62 h). UV-Vis (dmso/water 9:1), λ_{max}/nm ($\varepsilon/M^{-1}cm^{-1}$) = 317 ($8.2 \cdot 10^3$) (t = 5 min); 317 ($4.1 \cdot 10^3$) (t = 62 h). UV-Vis (dmso/water 1:1 + NaCl 0.1 M) = 317 ($8.3 \cdot 10^3$) (t = 5 min); 317 ($6.9 \cdot 10^3$) (t = 62 h). ^{1}H NMR (d6-dmso/D_2O 9:1): δ = 9.31 (s, **4a**), 9.04 (m, **LN**), 8.92 (d, **4a**), 8.75 (m, **LN**), 8.41 (d, **4a**), 8.24 (m, **LN**), 7.62 (m, **4a**), 7.54 (m, **LN**), 7.24 (d, **4a**), 7.16 (d, **LN**), 7.11 (d, **4a**), 7.09 (d, **LN**), 6.57 (d, **4b**), 6.39 (d, **4b**), 6.27 (d, **4b**), 6.15 (m, **4a**), 6.07 (d, **4b**), 6.06 (m, **4a**), 6.03 (s, **LN**), 5.96 (d, **4a**), 5.51 (s, **4a**), 5.48 (s, **LN**), 5.02 (s, **4a**), 4.50 (m-br, **4a** + **LN**), 4.26 (q, **4b**), 4.06 (q, **4a**), 2.43 (m, **4a**), 2.33 (q, **4a**), 2.25 (s, **4b**), 1.93 (s, **4a**), 1.15 (d, **4a**), 1.04 (t, **4a**). Ratio **4a** : **4b** : **LN** = 100:0:0 (t = 5 min), 45:50:55 (t = 24 h), 23:60:63 (t = 46 h), 17:65:67 (t = 62 h). ^{1}H NMR (d6-dmso/D_2O 1:1 + NaCl 0.1 M): **4a**, **4b**, and **4c** [δ = 8.92 (m), 8.64 (d), 8.21 (d), 7.49 (m), 7.01 (d), 6.92 (d), 6.97, 6.02, 5.98, 5.90, 5.41 (s), 4.91 (s), 2.01 ppm (s)]. Ratio 100:0:0 (t = 5 min), 100:31:11 (t = 24 h), 100:70:20 (t = 46 h), 100:100:20 (t = 62 h). **LN** is not soluble in these conditions. $^{13}C\{^1H\}$ NMR (d6-dmso/D_2O 9:1): δ = LN and **4a** [δ = 86.6, 83.8, 71.8, 51.3, 30.8, 22.2, 22.0, 18.6 ppm] (t = 62 h). ^{31}P NMR (d6-dmso/D_2O 9:1): δ = –76.5 (**4a**), –74.8 (**4b**) ppm. Ratio 100:0

(t = 2 h), 42:58 (t = 24 h), 23:76 (t = 46 h), 17:82 (t = 62 h). ^{31}P NMR (d6-dmso/D_2O 1:1 + NaCl 0.1 M): **4a**, **4b**, and **4c** [δ = –72.0 ppm]. Ratio 100:0:0 (t = 2 h), 64:35:0 (t = 24 h), 46:46:7 (t = 46 h), 35:47:12 (t = 62 h).

X-ray crystallography

Crystal data and collection details for **1** and **3**·CH_2Cl_2·½[1,4-$C_6H_4(OH)_2$] are reported in Table 4. X-ray data were collected on Bruker Smart APEX CCD (**3**) and Smart Apex CCD DUO (**1**) diffractometers equipped with a normal focus, 2.4 kW sealed tube source (Molybdenum radiation, λ = 0.71073 Å), operating at 50 kV and 30 (**1**) or 40 (**3**) mA. Data were collected over the complete sphere by a combination of four sets. Each frame exposure time was 30 s (**1**) or 10 s (**3**), covering 0.3° in ω. Data were corrected for absorption by using a multiscan method applied with the Sadabs program.[30] The structures were solved by the Patterson method or by direct methods. Refinement, by full-matrix least squares on F^2 with SHELXL97,[31] was similar for the two complexes, including isotropic and subsequently anisotropic displacement parameters. The hydrogen atoms were observed or calculated and refined freely, or using a restricted riding model. In the case of **3**, half molecule of hydroquinone (added to facilitate the crystallization, *vide infra*) and one molecule of dichloromethane were observed in the asymmetric unit. All the highest electronic residuals were observed in the close proximity of the Os centers and do not hold any chemical significance.

Table 4. Crystal data and measurement details for **1** and **3**·CH_2Cl_2·½[1,4-$C_6H_4(OH)_2$].

Complex	**1**	**3**·CH_2Cl_2·½[1,4-$C_6H_4(OH)_2$]
Formula	$C_{28}H_{32}Cl_2O_6Os$	$C_{35}H_{38}Cl_6NO_7Os$
FW	725.64	987.56
T, K	100(2)	100(2)
λ, Å	0.71073	0.71073
Crystal system	orthorhombic	monoclinic
Space group	*Pbca*	*P21/n*
a, Å	19.6723(19)	17.0370(17)
b, Å	11.5289(11)	13.3798(13)
c, Å	24.095(2)	17.2905(17)
β, °		103.3800(10)
Cell Volume, Å^3	5464.8(9)	3834.4(7)
Z	8	4

D_c, g·cm^{-3}	1.764	1.711
μ, mm^{-1}	4.903	3.791
F(000)	2864	1956
Crystal size, mm	0.10 x 0.09 x 0.06	0.19 x 0.10 x 0.06
θ limits, °	1.7 – 29.6	1.9 – 28.6
Reflections collected	57473	45640
Independent reflections	7332	9208
Data / restraints /parameters	7332 / 0 / 340	9208 / 4 / 457
Goodness of fit on F^2	1.011	1.001
R_1 ($I > 2\sigma(I)$)	0.0299	0.0389
wR_2 (all data)	0.0621	0.0821
Largest diff. peak and hole, e Å^{-3}	1.501, -1.111	1.146, -1.313

Cell culture

Human A2780 and A2780cisR ovarian carcinoma cells were obtained from the European Centre of Cell Cultures (ECACC, UK). Nontumorigenic HEK-293 cells were obtained from ATCC (Sigma, Switzerland). A2780 and A2780cisR were routinely grown in RPMI 1640 GlutaMAX (Lifetechnologies, Switzerland), while HEK-293 were grown in DMEM medium, both containing 10% heat-inactivated fetal bovine serum (FBS, Pan Biotech, Germany) and 1% antibiotics (penicillin/streptomycin), at 37 °C and CO_2 (5%).

Determination of antiproliferative activity

Cytotoxicity was determined using the MTT assay (MTT = 3-(4,5-dimethyl-2-thiazolyl)-2,5-diphenyl-2H-tetrazolium bromide). Cells were seeded in 96-well plates as monolayers with 100 μL of cell solution per well and pre-incubated for 24 h in the cell culture medium. Compounds were prepared as DMSO solutions that were rapidly dissolved in the culture medium and serially diluted to the appropriate concentration to give a final DMSO concentration of 0.5%. 100 μL of the drug solution were added to each well and the plates were incubated for another 72 h. Subsequently, MTT (5 mg/mL solution) was added to the cells and the plates were incubated for further 4 h. The culture medium was aspirated, and the purple formazan crystals formed by the mitochondrial dehydrogenase activity of vital cells were dissolved in DMSO. The optical density, directly proportional to the number of surviving cells, was quantified at 590 nm using a multiwell plate reader (Molecular Devices) and the fraction of

surviving cells was calculated from the absorbance of untreated control cells. Evaluation is based on means from three independent experiments, each comprising four testings per concentration level.

GST activity assay

A2780 and A2780cisR cells were plated in six well plates ($2x10^6$ cells/well) and incubated for 24 h in a CO_2 incubator at 37 °C. The cells were then exposed to compounds **LN**, **LP**, EA-(C=O)O$(CH_2)_2$OH, **1**–**4** for 18 h, at final concentrations according to the IC_{50} concentration for each respective cell line. The cells were then washed twice with PBS, harvested, lysed by a repetitive freeze–thaw cycle, and centrifuged at 10 000*g* for 15 min at 4 °C. The supernatants were used for the analysis of GST activity according to a fluorometric GST detection kit (Abnova). The changes in fluorescent intensities at Ex/Em 380/460 nm were recorded in a kinetic mode, every 5 min over 60 min, on a microplate reader (Molecular Devices). Two independent experiments were performed in which the GST activities were measured in duplicate. The GST activity expressed as U/min/mL per mg protein was converted to % activity of control (non-treated cells). The GST activity of the test samples was calculated by applying the equation $\Delta RFU = RFU_2 - RFU_1$ to the GST standard curve to get B [mU] during the reaction time ($\Delta T = T_2 - T_1$). The sample GST activity is calculated by the following formula: sample GST activity = $B/(\Delta T \times V) \times$ dilution factor [mU/min/mL], where B is sample GST activity from the GST standard curve [mU], ΔT is the reaction time (min), V is the sample volume added into the reaction well [mL].

Protein Determination

The protein concentration was determined by a Bradford assay (Bio-Rad) using BSA as a standard.

Corresponding Authors

*E-mail addresses: maester@unizar.es, fabio.marchetti1974@unipi.it.

Notes

The authors declare no competing financial interest.

Acknowledgement

We thank the *Swiss National Science Foundation*, *MINECO of Spain* (Projects CTQ2014-52799-P and CTQ2014-51912-REDC), the *Diputación General de Aragón* (E-35), the *European Social Fund* (FSE

and FEDER), and the *University of Pisa* (PRA 2015) for financial support. M. P. G. (FPI grant) thanks MINECO for funding.

Supporting Information Available

CCDC reference numbers 1421240 (**1**) and 1421241 (**3**) contain the supplementary crystallographic data for the X-ray studies reported in this paper. These data can be obtained free of charge at www.ccdc.cam.ac.uk/conts/retrieving.html (or from the Cambridge Crystallographic Data Centre, 12, Union Road, Cambridge CB2 1EZ, UK; fax: (internat.) +44-1223/336-033; e-mail: deposit@ccdc.cam.ac.uk).

References

1 a) Murray, B. S.; Babak, M. V.; Hartinger, C. G.; Dyson, P. J.; *Coord. Chem. Rev*., **2016**, *306*, 86–114. b) Hartinger, C. G.; Metzler-Nolte, N.; Dyson, P. J. *Organometallics* **2012**, *31*, 5677−5685. c) Peacock, A. F. A.; Sadler, P. J. *Chem. Asian J*., **2008**, *3*, 1890-1899. d) Hartinger, C. G.; Dyson, P. J. *Chem. Soc. Rev*., **2009**, *38*, 391-401. e) Cuesta, L.; Sessler, J. L. *Chem. Soc. Rev*., **2009**, *38*, 2716-2729.

2 a) Scolaro, A. Bergamo, L. Brescacin, R. Delfino, M. Cocchietto, G. Laurenczy, T. J. Geldbach, G. Sava, P. J. Dyson, *J. Med. Chem*., **2005**, *48*, 4161-4171. b) Bergamo, A. Masi, P. J. Dyson, G. Sava, *Int. J. Onco.*, **2008**, *33*, 1281-1289. c) Weiss, A.; Berndsen, R. H.; Dubois, M.; Müller, C.; Schibli, R.; Griffioen, A. W.; Dyson, P. J.; Nowak-Sliwinska, P. *Chem. Sci.*, **2014**, *5*, 4742-4748. d) Noffke, A. L.; Habtemariam, A.; Pizarro, A. M.; Sadler, P. J. *Chem. Commun*. **2012**, *48*, 5219-5246, *and references therein*. e) Bergamo, A., Masi, A., Peacock, A.F.A., Habtemariam, A., Sadler, P.J., Sava, G. J. *Inorg. Biochem*. **2010**, *104*, 79-86. f) Weiss, A.; Bonvin, D.; Berndsen, R. H.; Scherrer, E.; Wong, T. J.; Dyson, P. J.; Griffioen, A. W.; Nowak-Sliwinska, P. *Sci. Rep.* **2015**, *5*, 8990.

3 *Recent references include*: a) Filak, L. K.; Kalinowski, D. S.; Bauer, T. J.; Richardson, D. R.; Arion, V. B. *Inorg. Chem*. **2014**, *53*, 6934-6943. b) Kilpin, K. J.; Crot, S.; Riedel, T.; Kitchen, J. A.; Dyson, P. J. *Dalton Trans*. **2014**, *43*, 1443-1448. c) Fu, Y.; Soni, R.; Romero, M. J.; Pizarro, A. M.; Salassa, L.; Clarkson, G. J.; Hearn, J. M.; Habtemariam, A.; Wills, M.; Sadler, P. J. *Chem. Eur. J*. **2013**, *19*, 15199-15209. d) Romero-Canelon, I.; Salassa, L.; Sadler, P. J., *J. Med. Chem*. **2013**, *56*, 1291-1300. e) Fu, Y.; Romero, M. J.; Habtemariam, A.; Snowden, M. E.; Song, L.; Clarkson, G. J.; Qamar, B.; Pizarro, A. M.; Unwin, P. R.; Sadler, P. J. *Chem. Sci*. **2012**, *3*, 2485-2494. f) Shnyder, S. D.; Fu, Y.; Habtemariam, A.; van Rijt, S. H.; Cooper, P. A.; Loadman, P. M.; Sadler, P. J. *MedChemComm* **2011**, *2*, 666-668. g) Renfrew, A. K.; Phillips, A. D.; Egger, A. E.; Hartinger, C. G.; Bosquain, S. S.; Nazarov, A. A.; Keppler, B. K.; Gonsalvi, L.; Peruzzini, M.; Dyson, P. J. *Organometallics* **2009**, *28*, 1165–1172.

4 a) Wang, H.; DeYonker, N. J.; Gao, H.; Ji, L.; Zhao, C.; Mao, Z.-W., *J. Organomet. Chem*. **2012**, *704*, 17-28. b) Pizarro, A. M.; Habtemariam, A.; Sadler, P. J. *in Medicinal Organometallic Chemistry,* ed. G. Jaouen and N. Metzler-Nolte, Springer, Heidelberg, Dordrecht, London, New York, **2010**, *32*, 21–56. c) Fu, Y.; Habtemariam, A.; Pizarro, A. M.; van Rijt, S. H.; Healey, D. J.; Cooper, P. A.; Shnyder, S. D.; Clarkson, G. J.; Sadler, P. J., *J. Med. Chem.* **2010**, *53*, 8192-8196. d) Hanif, M.; Nazarov, A. A.; Hartinger, C. G.; Kandioller, W.; Jakupec, M. A.; Arion, V. B.; Dyson, P. J.; Keppler, B. K. *Dalton Trans*. **2010**, *39*, 7345-7352. e) Peacock, A. F. A.; Habtemariam, A.; Moggach, S. A.; Prescimone, A.; Parsons, S.; Sadler, P. J. *Inorg. Chem*. **2007**, *46*, 4049-4059.

5 a) Chari, R. V. J.; Miller, M. L.; Widdison, W. C. *Angew. Chem. Int. Ed.* **2014**, *53*, 3796-3827. b) Hanifa, M.; Meier, S. M.; Kandioller, W.; Bytzek, A.; Hejl, M.; Hartinger, C. G.; Nazarov, A. A.; Arion, V. B.; Jakupec, M. A.; Dyson, P. J.; Keppler, B. K. *J. Inorg. Biochem.* **2011**, *105*, 224-231.

c) N. Margiotta, N. Denora, R. Ostuni, V. Laquintana, A. Anderson, S. W. Johnson, G. Trapani, G. Natile, *J. Med. Chem*. **2010**, *53*, 5144-5154.

6 a) Kurzwernhart, A.; Kandioller, W.; Ba□chler, S.; Bartel, C.; Martic, S.; Buczkowska, M.; Mu□hlgassner, G.; Jakupec, M. A.; Kraatz, H.-B.; Bednarski, P. J. *J. Med. Chem.*, **2012**, *55*, 10512-10522. b) Kurzwernhart, A.; Kandioller, W.; Bartel, C.; Bächler, S.; Trondl, R.; Mühlgassner, G.; Jakupec, M. A.; Arion, V. B.; Marko, D.; Keppler, B. K. *Chem. Commun*., **2012**, *48*, 4839-4841. c) Kurzwernhart, A.; Kandioller, W.; Enyedy, É. A.; Novak, M.; Jakupec, M. A.; Keppler, B. K.; Hartinger, C. G. *Dalton Trans.*, **2013**, *42*, 6193-6202.

7 Kandioller, W.; Balsano, E.; Meier, S. M.; Jungwirth, U.; Goschl, S.; Roller, A.; Jakupec, M. A.; Berger, W.; Keppler, B. K.; Hartinger, C. G. *Chem. Commun.*, **2013**, *49*, 3348-3350.

8 (a) Arion, V. B.; Dobrov, A.; Goschl, S.; Jakupec, M. A.; Keppler, B. K.; *Chem. Commun*., **2012**, *48*, 8559-8561. (b) Muehlgassner, G.; Bartel, C.; Schmid, W. F.; Jakupec, M. A.; Arion, V. B.; Keppler, B. K. J. *Inorg. Biochem*. **2012**, *116*, 180-187.

9 Nazarov, A. A.; Meier, S. M.; Zava, O.; Nosova, Y. N.; Milaeva, E. R.; Hartinger, C. G.; Dyson, P. J. *Dalton Trans*., **2015**, *44*, 3614-23.

10 a) Ang, W. H.; Parker, L. J.; De Luca, A.; Juillerat-Jeanneret, L.; Morton, C. J.; Lo Bello, M.; Parker, M. W.; Dyson, P. J. *Angew. Chem. Int. Ed.* **2009**, *48*, 3854-3857. b) Wang, R.; Li, C.; Song, D.; Zhao, G.; Zhao, L.; Jing, Y. *Cancer Res*. **2007**, *67*, 7856-7864.

11 a) Nazarov, A. A.; Hartinger, C. G.; Dyson, P. J. *J. Organomet. Chem.*, **2014**, *751*, 251-260. b) Singh, A. K.; Pandey, D. S.; Xu, Q.; Braunstein, P. *Coord. Chem. Rev.*, **2014**, *270-271*, 31-56. c) Hartinger, C. G.; Phillips, A. D.; Nazarov, A. A. *Curr. Top. Med. Chem.*, **2011**, *11*, 2688-2702. d) Levina, A.; Mitra, A.; Lay, P.A. *Metallomics*, **2009**, *1*, 458-470. e) Gasser, G.; Ott, I.; Metzler-Nolte, N. *J. Med. Chem.*, **2011**, *54*, 3-25.

12 Ang, W. H.; De Luca, A.; Chapuis-Bernasconi, C.; Juillerat-Jeanneret, L.; Lo Bello, M.; Dyson, P. J. *ChemMedChem*, **2007**, *2*, 1799-1806.

13 Agonigi, A.; Riedel, T.; Zacchini, S.; Păunescu, E.; Pampaloni, G.; Bartalucci, N.; Dyson, P. J.; Marchetti, F. *Inorg. Chem*., **2015**, 54, 6504–6512.

14 a) Ang, W. H.; Khalaila, I.; Allardyce, C. S.; Juillerat-Jeanneret, L.; Dyson, P. J. *J. Am. Chem. Soc.*, **2005**, *127*, 1382-1383. b) Parker, L. J.; Italiano, L. C.; Morton, C. J.; Hancock, N. C.; Ascher, D. B.; Aitken, J. B.; Harris, H. H.; Campomanes, P.; Rothlisberger, U.; De Luca, A.; Lo Bello, M.; Ang, W.-H.; Dyson, P. J.; Parker, M. W. *Chem. Eur. J.*, **2011**, *17*, 7806-7816.

15 a) Chatterjee, S.; Biondi, I.; Dyson, P. J.; Bhattacharyya, A.; *J. Biol. Inorg. Chem.*, **2011**, *16*, 715-724. b) Johansson, K.; Ito, M.; Schophuizen, C. M. S.; Thengumtharayil, S. M.; Heuser, V. D.; Zhang, J.; Shimoji, M.; Vahter, M.; Ang, W. H.; Dyson, P. J.; Shibata, A.; Shuto, S.; Ito, Y.; Abe, H.; Morgenstern, R. *Mol. Pharmaceutics*, **2011**, *8*, 1698-1708.

16 Michelman, R. I.; Ball, G. E.; Bergman, R. G.; Andersen, R. A. *Organometallics* **1994**, *13*, 869-881.

17 Darensbourg, D. J.; Robertson, J. B.; Larkins, D. L.; Reibenspies, J. H., *Inorg. Chem*. **1999**, *38*, 2473-2481.

18 Dorcier A.; Dyson P. J.; Gossens C.; Rothlisberger U.; Scopelliti R.; Tavernelli I. *Organometallics* **2005**, *24*, 2114-2123.

19 Dorcier, A.; Hartinger, C. G.; Scopelliti, R.; Fish, R. H.; Keppler, B. K.; Dyson, P. J. *J. Inorg. Biochem.*, **2008**, *102*, 1066–1076.

20 a) Horikoshi, R.; Nambu, C.; Mochida, T. *New. J. Chem.* **2004**, *28*, 26-33. b) Sridhar, B.; Nanubolu, J. B.; Ravikumar, K. *Acta Cryst*., **2015**, C71, 602-609.

21 a) Carmona, D.; Lahoz, F. J.; García-Orduñ, P.; Oro, L. A.; Lamata, M. P.; Viguri, F. *Organometallics* **2012**, *31*, 3333-3345. b) Esteruelas, M. A.; García-Yebra, C.; Oliván, M.; Oñate,

E.; Valencia. M. *Organometallics* **2008**, *27*, 4892-4902. c) Godó, A. J.; Bényei, A.; Duff, B.; Egan, D. A.; Buglyó, P. *RSC Adv.*, **2012**, *2*, 1486-1495. d) Peacock, A. F. A.; Melchart, M.; Deeth, R. J.; Habtemariam, A.; Parsons, S.; Sadler, P. J. *Chem. Eur. J.* **2007**, *13*, 2601-2613.

22 Lamotre, P. J.; Campsteyn, H.; Dupont, L.; Vermeire, M. *Acta Cryst.,* **1978**, *B34*, 2636-2638.

23 a) van Rijt, S. H.; Peacock, A. F. A.; Johnstone, R. D. L.; Parsons, S.; Sadler, P. J. *Inorg. Chem.* **2009**, *48*, 1753-1762. b) Cheng, Y.-M.; Li, E. Y.; Lee, G.-H.; Chou, P.-T.; Lin, S.-Y.; Shu, C.-F; Hwang K.-C., Chen, Y.-L.; Song, Y.-H.; Chi, Y. *Inorg. Chem.* **2007**, *46*, 10276-10286. c) Esteruelas, M. A.; Garcìa-Yebra, C.; Oliván, M.; Oňate, E.; Tajada, M. A. *Organometallics* **2000**, *19*, 5098-5106. c) Otto, M.; Parr, J.; Slawin, A. M. Z. *Organometallics* **1998**, *17*, 4527-4529.

24 a) Peacock, A. F. A.; Habtemariam, A.; Fernandez, R.; Walland, V.; Fabbiani, F. P. A.; Parsons, S.; Aird, R. E.; Jodrell, D. I.; Sadler, P. J. *J. Am. Chem. Soc.* **2006**, *128*, 1739-1748. b) Bennett, M. A.; Mitchell, T. R. B.; Stevens, M. R.; Willis A. C. *Can. J. Chem.* **2001**, *79*, 655-669.

25 Kilpin, K. J.; Clavel, C. M.; Edafe, F.; Dyson, P. J. *Organometallics,* **2012**, *31*, 7031-7039.

26 Cynkowska, G.; Cynkowski, T.; Al-Ghananeem, A. A.; Guo, H.; Ashton, P.; Crooks, P. A. *Bioorg. Med. Chem. Lett.*, **2005**, *15*, 3524–3527.

27 E. Păunescu, P. Nowak-Sliwinska, C. M. Clavel, R. Scopelliti, A. W. Griffioen, P. J. Dyson, ChemMedChem, 2015, 10, 1539 – 1547.

28 Castarlenas R.; Esteruelas M. A.; Oñate E. Organometallics 2005, 24, 4343-4346.

29 a) Jutand, A. *Eur. J. Inorg. Chem*., **2003**, 2017-2040. b) Geary, W. J. *Coord. Chem. Rev.*, **1971**, *7*, 81-122.

30 a) Blessing, R. H. *Acta Cryst*. **1995**, *A51*, 33-38. b) SADABS: Area-detector absorption correction; Bruker- AXS, Madison, WI, **1996**.

31 a) SHELXTL Package v. 6.14; Bruker-AXS, Madison, WI, **2000**. b) Sheldrick, G. M. *Acta Cryst.* **2008**, *A64*, 112-122.

Table of Contents Synopsis and graphic

The first examples of osmium complexes containing ethacrynic acid modified ligands were prepared and their in vitro anticancer activity and intracellular glutathione S-transferase inhibition activity investigated.